



# 3D-reconstructions and virtual 4D-visualization to study metamorphic brain development in the sphinx moth *Manduca sexta*

Wolf Huetteroth<sup>††</sup>, Basil el Jundi<sup>†</sup>, Sirri el Jundi and Joachim Schachtner\*

Department of Biology, Animal Physiology, Philipps-University Marburg, Marburg, Germany

## Edited by:

Randolf Menzel, Freie Universität Berlin, Germany

## Reviewed by:

Hanna Mustaparta, Norwegian University of Science and Technology, Norway

John Hildebrand, University of Arizona, USA

## \*Correspondence:

Joachim Schachtner, Department of Biology, Animal Physiology, Philipps-University Marburg, Karl-von-Frisch-Str. 8, D-35032 Marburg, Germany.  
e-mail: schachtj@staff.uni-marburg.de

## †Present address:

Wolf Huetteroth, Department of Neurobiology, University of Massachusetts Medical School, Worcester, MA, USA

<sup>††</sup>Wolf Huetteroth and Basil el Jundi contributed equally.

During metamorphosis, the transition from the larva to the adult, the insect brain undergoes considerable remodeling: new neurons are integrated while larval neurons are remodeled or eliminated. One well acknowledged model to study metamorphic brain development is the sphinx moth *Manduca sexta*. To further understand mechanisms involved in the metamorphic transition of the brain we generated a 3D standard brain based on selected brain areas of adult females and 3D reconstructed the same areas during defined stages of pupal development. Selected brain areas include for example mushroom bodies, central complex, antennal- and optic lobes. With this approach we eventually want to quantify developmental changes in neuropilar architecture, but also quantify changes in the neuronal complement and monitor the development of selected neuronal populations. Furthermore, we used a modeling software (Cinema 4D) to create a virtual 4D brain, morphing through its developmental stages. Thus the didactical advantages of 3D visualization are expanded to better comprehend complex processes of neuropil formation and remodeling during development. To obtain datasets of the *M. sexta* brain areas, we stained whole brains with an antiserum against the synaptic vesicle protein synapsin. Such labeled brains were then scanned with a confocal laser scanning microscope and selected neuropils were reconstructed with the 3D software AMIRA 4.1.

**Keywords:** animation, brain, development, digital neuroanatomy, insect, *Manduca*, neuropil

## INTRODUCTION

Brains are typically organized in defined neuropils, which can usually be characterized by their spatial location, gross anatomy, and often by a certain function and brains of evolutionary related animals typically share a similar neuroarchitecture. During development, the formation of brain neuropils including their location and interconnections follows a minute pattern in time and space orchestrated by complex (genetical) programs which eventually give rise to the adult brain structures.

Metamorphosis, the transition of a larva to an adult insect has always fascinated us humans. By far, most of the living insects belong to the group of holometabolous insects (Grimaldi and Engel, 2005) which have in addition to the embryonic development a second developmental phase called metamorphosis. During metamorphosis, as demonstrated by many researchers over the years, the nervous system undergoes considerable remodeling: new neurons are integrated while larval neurons are remodeled or eliminated (for reviews see e.g. Truman, 1996, 2009). Most obvious, neuropils involved in the processing of visual and olfactory information are to a large extent newly formed during metamorphosis. To understand further the mechanisms involved in transforming a larval to an adult brain, we have mapped the anatomical changes of selected brain areas throughout metamorphosis of the sphinx moth *Manduca sexta*. *M. sexta* serves since long as a model to understand metamorphic brain development and the development of most of the discernable brain areas has been described earlier (see Discussion). However, so far a comprehensive view which compares

the anatomical changes of all these brain neuropils throughout metamorphic development is missing. Thus, the aim of the current study was to visualize the anatomical changes of discernable brain areas in parallel and thus to provide a tool which allows a comparison of these changes along the developmental time line.

To obtain the desired datasets, we labeled whole brains of different metamorphic stages with an antiserum against the synaptic vesicle protein synapsin to visualize neuropil areas, analyzed the staining using confocal laser scanning microscopy, 3D reconstructed the selected brain neuropils using the software AMIRA (Visage Imaging, Fürth, Germany), and subsequently transformed the data sets into the 4D visualization software Cinema 4D. The used technique can in principal be adapted to any brain area which can be visualized and 3D reconstructed at different times of development.

## MATERIALS AND METHODS

### ANIMALS

Moths (*M. sexta*; Lepidoptera: Sphingidae) were raised at 26°C under a long-day photoperiod (L:D = 17:7) and were fed on an artificial diet (Bell and Joachim, 1978). Under these conditions animals required 18 days from hatching to pupal ecdysis and another 20 days from pupal ecdysis to adult eclosion. The wandering stage presents the last phase of the fifth larval stage (L5) and consists of about 5 days (W0–W4). The beginning of this stage (W0) is characterized by the occurrence of a red pigment along the dorsal vessel. At about noon of W2, the animals go into a quiescent

prepupal stage. Pupal ecdysis occurs on day W4, and the newly formed pupa is designated as day P0. Subsequent days of pupal development are counted as P1–P20. The freshly eclosed adult individual is termed A0. The staging of larvae and pupae was based on the criteria described by Schwartz and Truman (1983) and Jindra et al. (1997). For our experiments we used only female animals.

To describe, visualize and animate the development of the brain of *M. sexta* during pupal metamorphosis we 3D-reconstructed brains from defined pupal stages. We reconstructed two brains of representative stages (except stage P4;  $n = 1$ ), including the fifth instar larva (L5) and nine pupal stages during metamorphosis (P0; P1; P3; P4; P7; P9; P11; P14; P16). As adult brain we used the *M. sexta* standard brain (freshly eclosed, A0) for our animation (el Jundi et al., 2009).

### IMMUNOHISTOCHEMISTRY

For our studies we used a wholemount staining protocol as described in el Jundi et al. (2009). Brains from different developmental stages were dissected out of the head capsule under cold saline (Weevers, 1966) and were fixed overnight at 4°C, in a solution composed of one part formaldehyde (37%, Roth, Karlsruhe, Germany), one part methanol and eight parts phosphate-buffered saline (PBS 0.01 M, pH 7.4). Whole brains were rinsed in 0.1 M PBS containing 0.3% Triton X-100 (PBT) for 1 h at room temperature and were preincubated (4°C, overnight) in 5% normal goat serum (NGS; Jackson ImmunoResearch, Westgrove, PA, USA) in 0.1 M PBT containing 0.02% sodium azide. For visualization of the brain areas we used a monoclonal primary antibody from mouse against a fusion protein consisting of a glutathione-S-transferase and the first amino acids of the presynaptic vesicle protein synapsin I coded by its 5'-end (SYNORF1, Klagges et al., 1996, kindly provided by Dr. E. Buchner, Würzburg). Its specificity in *M. sexta* was shown in western blots by Utz et al. (2008). The anti-synapsin antibody was diluted 1:50 in 0.1 M PBT containing 1% NGS and 0.02% sodium azide.

After 4–6 days incubation with the primary antibody, the brains were rinsed 6 times in 2 h with PBT before they were incubated with the secondary goat anti-mouse antibody conjugated to Cy5 (1:300; Jackson ImmunoResearch, Westgrove, PA, USA) in PBT and 1% NGS for 4 days at 4°C. Afterwards, the brains were rinsed with PBT 6 times in 2 h, then dehydrated in an ascending ethanol series (50–100%, 15 min each) and then cleared in methyl salicylate (Merck, Gernsheim, Germany) for about 40 min. At last the brains were mounted in Permount (Fisher Scientific, Pittsburgh, PA, USA) between two coverslips. Compression of brains was prevented by spacers (Zweckform, Oberlaindern, Germany). According to the brain sizes we used for larval brains (L5) and early pupal brains three to five spacers (P0–P4). Late pupal brains (P7–P16) were embedded using six to nine spacers.

### IMAGE ACQUISITION

All brains were scanned with a confocal laser scanning microscope (Leica TCS SP2). The fluorescent signal of Cy5 was detected with a HeNe laser (633 nm). Late pupal brains (P7–P16) were imaged at  $512 \times 512$  pixel resolution by using a 10× oil immersion objective (HC PL APO 10×/NA: 0.40 Imm (working distance: 0.36 mm); Leica, Bensheim, Germany). Larval and early pupal brains (L5–P4) were scanned with a 10× oil objective or a 20× oil objective (HC PL

APO 20×/0.70 Imm Corr CS, Leica, Bensheim, Germany). All brains were scanned with a voxel size of  $2.9 \times 2.9 \mu\text{m}$  in xy-direction. Late pupal brains were imaged with a step size of  $2 \mu\text{m}$ , younger brains were detected with a step size of  $1.5 \mu\text{m}$ . The thickness of older brains and the limited working distance of the objectives made it necessary to scan the brains from two sides (anterior and posterior) to eventually acquire images of the whole brain. Younger brains were scanned only from anterior. Depending on xy dimension which increased with the developmental stage the brains had to be scanned in two and up to eight image stacks. For example, for P16 brains we needed three stacks from anterior and another three stacks from the posterior side. For A0 brains four stacks from each side were needed (el Jundi et al., 2009).

### IMAGE PROCESSING AND 3D RECONSTRUCTION

Image processing and 3D reconstruction were performed in the program AMIRA 4.1 (Visage Imaging, Fürth, Germany). First the different image stacks of all brain regions were merged into one stack: corresponding optical slices in the z direction in overlapping parts of the image stacks were found with the module *AlignSlices*, redundant slices of the stacks were abolished and corresponding batches of data were merged with the module *AlignSlices*. Before we merged these image stacks in xy direction, computation limits made it necessary to downsample the voxel size of the image stacks of P7–P16 pupal brains with the module *Resample* to a voxel size of  $6 \times 6 \times 6 \mu\text{m}$ . For brains < P7 it was not essential to downsample the image stacks. Again, we used the module *AlignSlices* for finding the corresponding optical slice and with the module *Merge* batches of data were merged into one batch of data which contained the whole brain.

For 3D reconstructions, *Labelfield* files were created with the same dimensions (voxel size, resolution) as the corresponding merged image stacks. Using the *Segmentation Editor*, reconstructions of selected neuropils were performed. Regions of interests were labeled in three dimensions in several optical slices and subsequently extrapolated into 3D structures by using the tool *Wrap*. Clearly identifiable neuropilar borders in all three dimensions based on anti-synapsin staining were the limiting criterion for reconstructing a brain region in a certain developmental stage. The color codes for neuropils are consistent with existing standard brain models (Brandt et al., 2005; Kurylas et al., 2008; el Jundi et al., 2009; Dreyer et al., 2010). With the module *SurfaceGen* the 3D surface visualizations were calculated. Based on visual appearance, surface models of brains which represented the according stage best were used for 4D visualization of the brain development during the metamorphosis.

### 4D VISUALIZATION

To animate the development of the brain of *M. sexta* during metamorphosis we reconstructed brains ranging from the last larval stage (L5) to brains of freshly eclosed animals (A0). Because of the limited computational capacity it was necessary to reduce the number of the polygons of the surface models in AMIRA. Subsequently, representative brains of distinct developmental stages were exported from Amira as drawing exchange format (.dxf) files and were opened in the software Cinema 4D (v.10.1; MAXON Computer, Friedrichsdorf, Germany). Only those brains

were chosen which clearly exhibited representative features of their stage. Using those brain polygon models as templates, the 4D visualization of brain development was created in Cinema 4D. The creation of the 4D visualization of the *M. sexta* brain is described in detail in the results.

## RESULTS

### ANATOMICAL DEVELOPMENT OF THE BRAIN NEUROPILS

Overall, we reconstructed 19 female brains from 10 different stages during *M. sexta* brain development. In an earlier study we already reconstructed 12 brains of freshly eclosed adult females (A0) to produce a standard brain (el Jundi et al., 2009). Since we wanted to cover the brain transition between the larval and the adult brain during pupal development, we started with fifth instar larval brains, chose nine stages during pupal development (P0, P1, P3, P4, P7, P9, P11, P14, P16) and closed with the female A0 standard brain (el Jundi et al., 2009). Because early metamorphic development coincides with more obvious structural changes, these phases were resolved with higher temporal resolution. During the approximately 3 weeks of pupal development, the *Manduca* brain undergoes an enormous increase in size (the reconstructed neuropils grow about 132-fold from P0 to A0), which is largely due to the development of the optic lobes (Figure 1). But all other parts of the brain also increase in size, and further developmental processes in the brain take place (Figures 2–6). Most prominently, the subesophageal ganglion merges with the supraesophageal ganglion, thereby forming the esophageal foramen. This process is initiated during the wandering stage and is finished around P3 (Amos and Mesce, 1994; Homberg and Hildebrand, 1994). Additionally, the metamorphosing brain undergoes certain rotational movements, mirrored in the orientation of neuropils in the brain: (1) Neuropils located anteriorly move upwards (mushroom body lobes, antennal lobes), (2) the brain midline folds slightly outwards towards the dorsal side (orientation of mushroom body calyces), and (3) central parts of the protocerebrum tilt back (mushroom body peduncles with calyces, central complex). Most of these movements are finished until P7/8, followed by further size increase of all neuropils. Because these movement and growth processes are temporally overlapping we created a 4D movie for better comprehension (see below; Movie S1 in Supplementary Material). Below, all major neuropils are dealt with in more detail.

#### The optic lobes

In the last larval stage (5th instar; L5), the larval optic center (LOC), is barely separated from the midbrain neuropil (Figure 1, gray line). The inner (IOA) and outer optic anlagen (OOA), the precursors of the adult optic neuropils, are already present, although they exhibit almost no anti-synapsin immunoreactivity at this stage. At this early stage, the accessory medulla (aMe) is still part of the LOC. Several other neuropils are already distinguishable, the larval antennal lobe (see Figure 2), the calyx (Ca) and peduncle (Pe) of the mushroom body (see Figure 3), and the protocerebral bridge (PB; see Figure 4). With the onset of pupation (P0), the optic lobe neuropils begin to grow and the now ribbon-like neuropils lamina (La), medulla (Me) and lobula (Lo) begin to show faint anti-synapsin staining. At this stage, the aMe is separated from the midbrain neuropil and stays close to the antero-medial rim of the Me. At P3 the outer

optic neuropils further expand mainly along the antero-posterior axis; the dorsal and ventral tips of the La bend behind the Me, thus resembling a horseshoe. The lobula plate (LoP) appears as a discernible structure between Me and Lo. The anti-synapsin staining gains intensity in all neuropils; the different layers of the Me become recognizable (Figure 1C'). After one third of pupal development (P7), the inner and outer lobula subunits (Loi, Loo) can be separated based on their anti-synapsin immunoreactivity. The La starts to exhibit its bowl-like appearance, the opening still tilted towards the anterior side. Three subunits of the anterior optic tubercle (AOTu, see Figure 5) are now present in the antero-dorsal protocerebrum. After two-thirds of pupal development (P14) all neuropils of the optic lobe reached their relative position and continue to increase in size until adult eclosion. The relative distance between La and Me increased up to here.

#### The antennal lobes

The primary larval integration site for olfactory information, the larval antennal center (LAC) exhibits no glomerular organization in *M. sexta* (Figure 2). The anti-synapsin staining resembles throughout AL development the anti-synaptotagmin staining described earlier (Dubuque et al., 2001). At P4 the developing AL becomes first visible with the anti-synapsin staining. Note the ventral position of the AL, even with the complete subesophageal ganglion fused to the supraesophageal ganglion. From P7, spheroidal structures, the forming olfactory glomeruli become visible in the developing AL. The glomeruli enclose a central coarse neuropil. The whole AL gains volume and wanders in a more antero-dorsal position. At P9, single glomeruli become clearly discernible within the AL. The dorsal migration of the whole AL slows down and eventually stalls. The volume curve indicates for the AL three developmental phases, which correspond to earlier studies (Figure 7; Oland and Tolbert, 1996; Dubuque et al., 2001; see Discussion).

#### The mushroom bodies

The larval (L5) mushroom body (MB) is characterized by rather thin  $\alpha$ - and  $\beta$ -lobes ( $\alpha$ L,  $\beta$ L) and a slender peduncle (Figure 3). The peduncle in the larva is still oriented antero-ventrally, with a slight inclination of the calyces (Ca) to the dorsal midline. While the  $\alpha$ L points antero-dorsally, the  $\beta$ L extends medially in the horizontal plane. Between stages P1 and P3 the pedunculi bend nearly 90 degree sideways and the whole MB starts to rotate backwards from a ventro-dorsal orientation to an antero-posterior orientation (Figure 6; Movie S1 in Supplementary Material). This rotation continues until P7, now the whole MB is oriented antero-posteriorly. Additionally to the  $\alpha$ L and  $\beta$ L, the  $\gamma$ -lobe ( $\gamma$ L) and the Y-lobe (YL, see in Figures 3D–D'', E–E'') can now be discerned.

#### Other neuropils of the CNS

Both central body (CB) and protocerebral bridge (PB) are recognizable structures in the larva already (L5, Figure 4). Based on anti-synapsin-immunoreactivity, the PB consists of two separate neuropils and retains this layout up to adulthood. At P3, the two parts of the PB elongate horizontally and also undergo the two main movements in the central brain (see Figure 3). The CB thickens, but shows no signs of subdivisions. At P7 the two subdivisions of the CB, the lower (CBL) and upper (CBU) subunit can be discerned. Since the CB

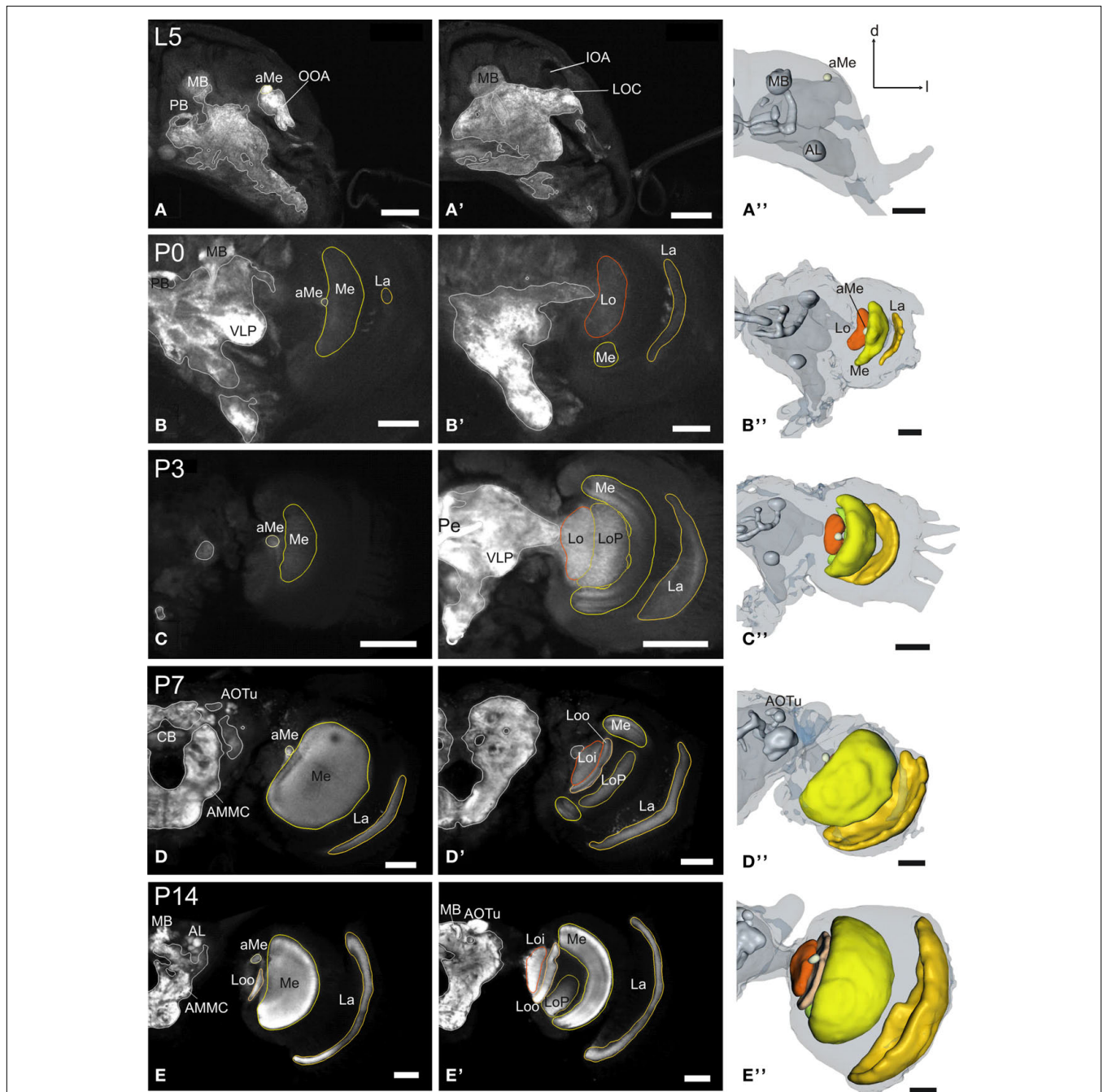


**FIGURE 1 | Development of the adult optic lobe.** Single optical sections in the frontal plane at different depths, anti-synapsin immunostaining (left two columns). Right column, 3D reconstructions (frontal views). **(A–A’)** Last larval stage (L5): the larval optic center (LOC) is hardly distinguishable from the midbrain neuropil (gray line). The accessory medulla (aMe) is part of the LOC. IOA, inner optic anlage; OOA, outer optic anlage. **(B–B’)** Stage P0: the ribbon-like adult neuropils lamina (La), medulla (Me) and lobula (Lo) show faint anti-synapsin staining. The aMe is separated from the midbrain neuropil and stays close to the antero-medial rim of the Me. Note the strong anti-synapsin

immunoreactivity in the ventrolateral protocerebrum (VLP). **(C–C’)** Stage P3: the La and Me further expand and the dorsal and ventral tips of the La bend behind the Me. The lobula plate (LoP) appears between Me and Lo. The anti-synapsin staining gains intensity in all neuropils; layers of the Me become recognizable. **(D–D’)** Stage P7: the inner and outer lobula (Loi, Loo) can be separated. The La starts to exhibit its bowl-like appearance, the opening still tilted towards the anterior side. **(E–E’)** Stage P14: all optic lobe neuropils reached their final adult positions. Orientation bars: d, dorsal; l, lateral; scale bars: 100 μm **(A–B’)**; 200 μm **(C–E’)**.

also underwent the rotation of the brain, the CBL is – now counter intuitively – in an antero-dorsal position to the CBU. The noduli (No) appear antero-ventrally to the CB. The two halves of the PB

grow closer together, but stay untouched. Their lateral ends now point postero-ventrally in their final orientation. After P7 the central complex remains in its position and undergoes further size increase.

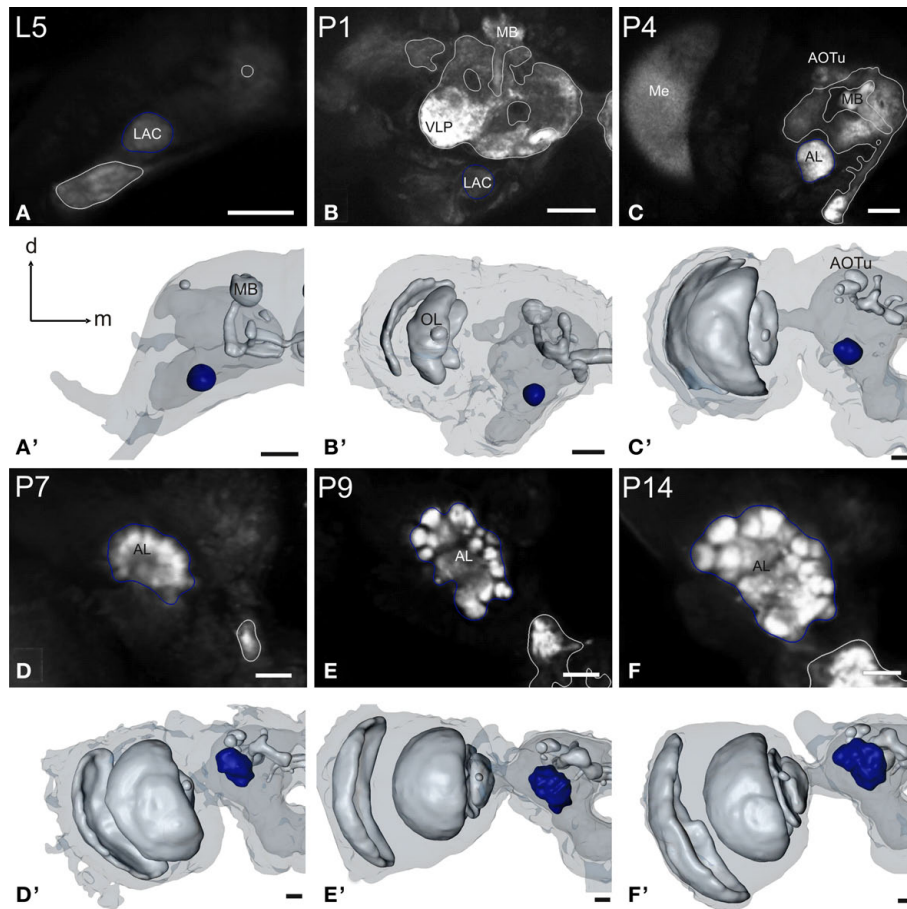


**FIGURE 2 | Development of the antennal lobe.** Single optical sections in the frontal plane, anti-synapsin immunostaining (first and third row). Second and fourth row, 3D reconstructions (frontal views). **(A–A')** The larval antennal center (LAC) exhibits no glomerular organization in *Manduca sexta* L5 larva. **(B–B')** Strong anti-synapsin immunoreactivity is visible in the ventro-lateral protocerebrum (VLP), compared to the weak labeling in the LAC/AL. **(C–C')** Stage P4: the developing AL becomes recognizable in the

anti-synapsin staining. Note the ventral position of the AL compared to stage P7. **(D–D')** Stage P7: glomerular structures surrounding a coarse neuropil become first visible. **(E–E')** Stage P9: single glomeruli become discernible structures and achieve their final position within the AL. The dorsal migration of the AL ends. **(F–F')** Stage P14: glomerular and AL volume increased compared to stage P9. Orientation bars: d, dorsal; m, medial; all scale bars: 100  $\mu\text{m}$ .

The larval brain houses no anterior optic tubercle (AOTu, not shown), its three subcompartments become discernible structures in the antero-dorso-lateral midbrain around P4 (**Figure 5**): the upper (uAOTu), lower (lAOTu), and the nodular subunit (nAOTu). Also the characteristic four nodules of the nAOTu become visible at the same time (**Figure 5A**). Interestingly, the brain rotation events around P7 leave all subunits of the AOTu relatively untouched; they remain in their position and increase in size. Further increasing in size, the uAOTu remains the largest subunit throughout metamorphic development.

The antennal mechanosensory and motor center (AMMC) is another neuropil region in the developing brain, but did not fulfill the criterion of clearly identifiable borders in all three dimensions, thus we refrained from including it into our reconstructions. The same is true for several other brain regions; most noteworthy are the dorsal and lateral protocerebrum. No clear-cut boundaries make a judgment on their developmental size increase and potential rotational movements rather ambiguous.

In general, these brain regions tend to be underrepresented in the literature. This is a well-known problem of brain anatomy and has recently been addressed in the fruit fly (Otsuna and Ito, 2006).

#### TIME COURSE OF NEUROPIL DEVELOPMENT

The anti-synapsin based immunostainings clearly show different time scales for the development of the various neuropils (**Figure 8**). Most neuropils including the aMe, the MB, the central body, and the protocerebral bridge were already present in the 5th larva. These neuropils changed during pupal development by (1) becoming more differentiated (e.g. the MBs obtain two additional lobes), (2) change of position (e.g. rotation of the MB), and (3) increase of volume. Other neuropils including the compartments of the optic lobes and the noduli are newly formed during this process. In the case of the first integration center for olfactory information, the LAC gets replaced by the AL (Kent et al., 1987; Jefferis et al., 2004).

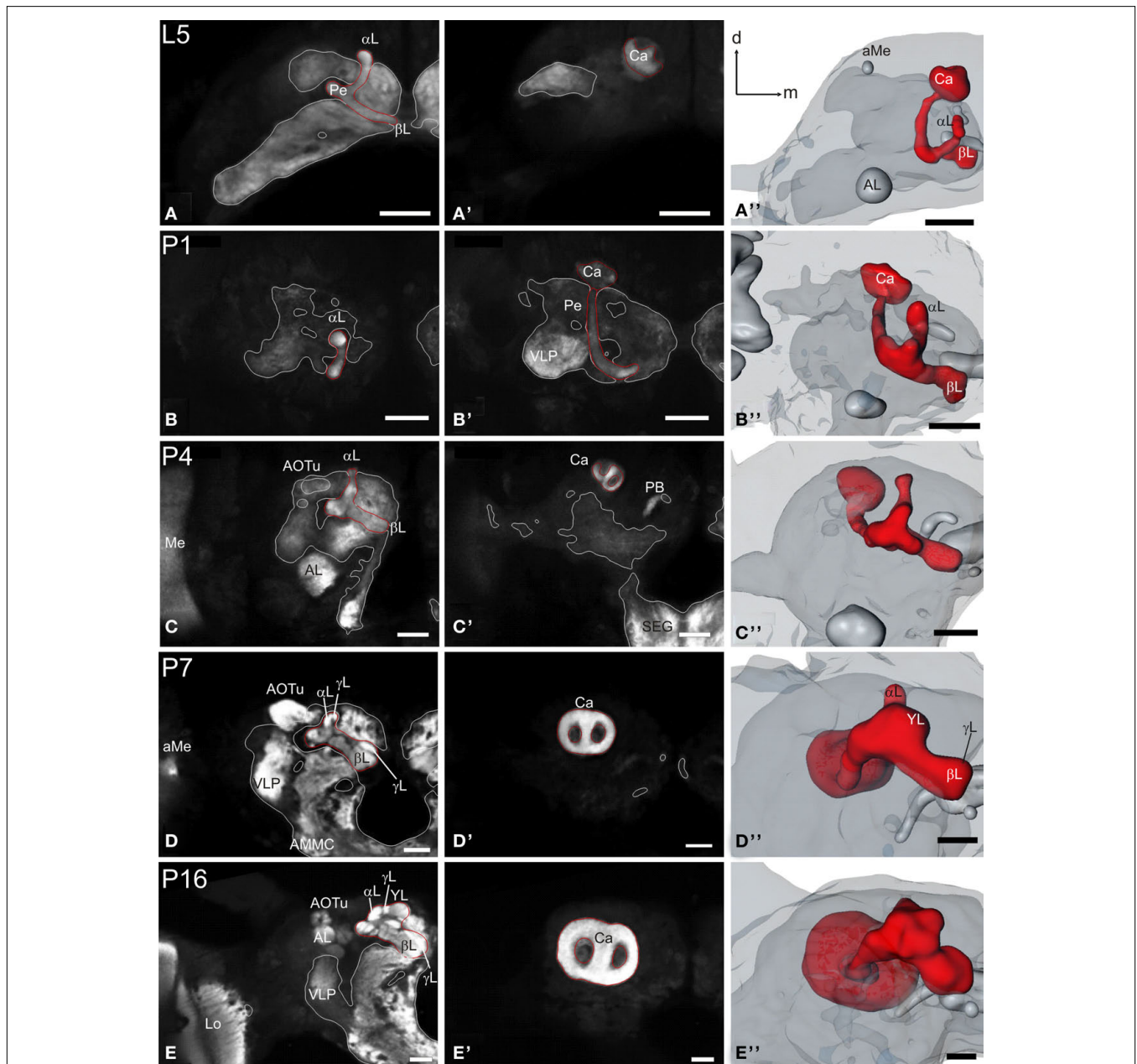
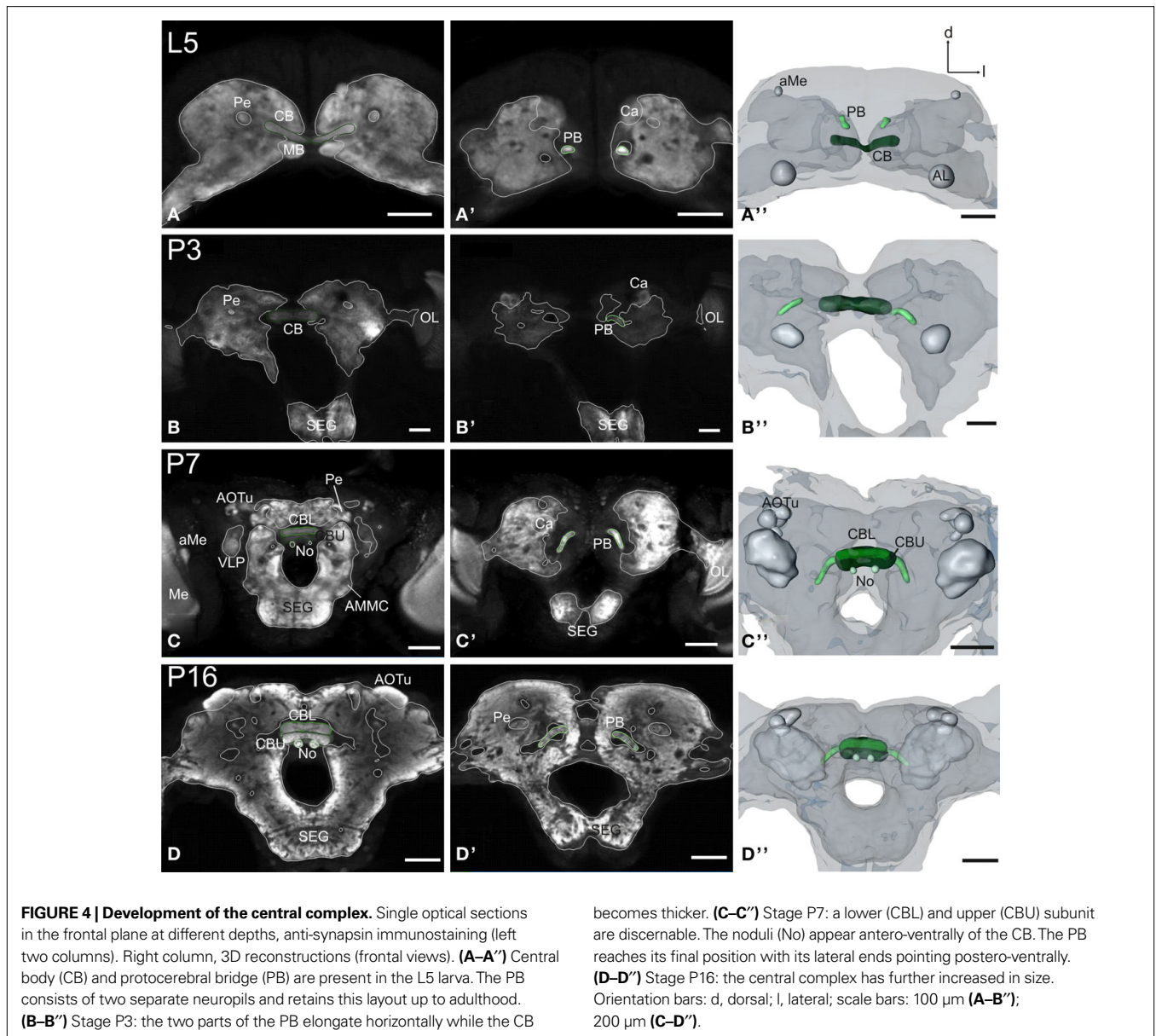


**FIGURE 3 | Development of the mushroom body.** Single optical sections in the frontal plane at different depths, anti-synapsin immunostaining (left two columns). Right column, 3D reconstructions (frontal views). **(A–A’)** Rather thin  $\alpha$ - and  $\beta$ -lobes ( $\alpha$ L,  $\beta$ L) and a slender peduncle are characteristic for the larval (L5) mushroom body (MB). The peduncle of the larval MB is oriented antero-ventrally, with a slight inclination of the calyces (Ca) to the dorsal midline. While the  $\alpha$ L points antero-dorsally, the  $\beta$ L extends medially in the horizontal plane. **(B–B’)** early pupae

**(P1):** the peduncle shows a straightened orientation. **(C–C’)** Stage P4: the MB tilts from a ventro-dorsal orientation to a more antero-posterior orientation. **(D–D’)** Stage P7: the MB is oriented antero-posteriorly and has massively increased in size compared to stage P4. Additionally to the  $\alpha$ L and  $\beta$ L, the  $\gamma$ -lobe ( $\gamma$ L) and the Y-lobe (YL) appear as protrusions on the MB. **(E–E’)** Stage P16: the MB reached its final adult orientation and shape. Orientation bars: d, dorsal; m, medial; all scale bars: 100  $\mu$ m.

The first wave of new neuropil development already starts in the larval stage including most neuropils of the optic lobe (La, Me, Loi). Those neuropils are laid out in the inner and outer optic anlagen, which slowly acquire anti-synapsin staining during continuous growth in the early pupal stages. The lobula plate and the AMMC gradually appear with the onset of pupal development, whereas the noduli and the subunits of the AOTu are not seen before P4 (Figure 8).

Between P4 and P7 the last structures which were included in this study appeared as separate neuropils. All are without exception subdivisions of already existing neuropils: the outer lobula separates from the inner lobula, the  $\gamma$ - and Y-lobe protrude from the mushroom body lobes, and the lower unit of the central body becomes discernible. Basically, after one third of metamorphic development all examined neuropils are already present. The ongoing two-thirds



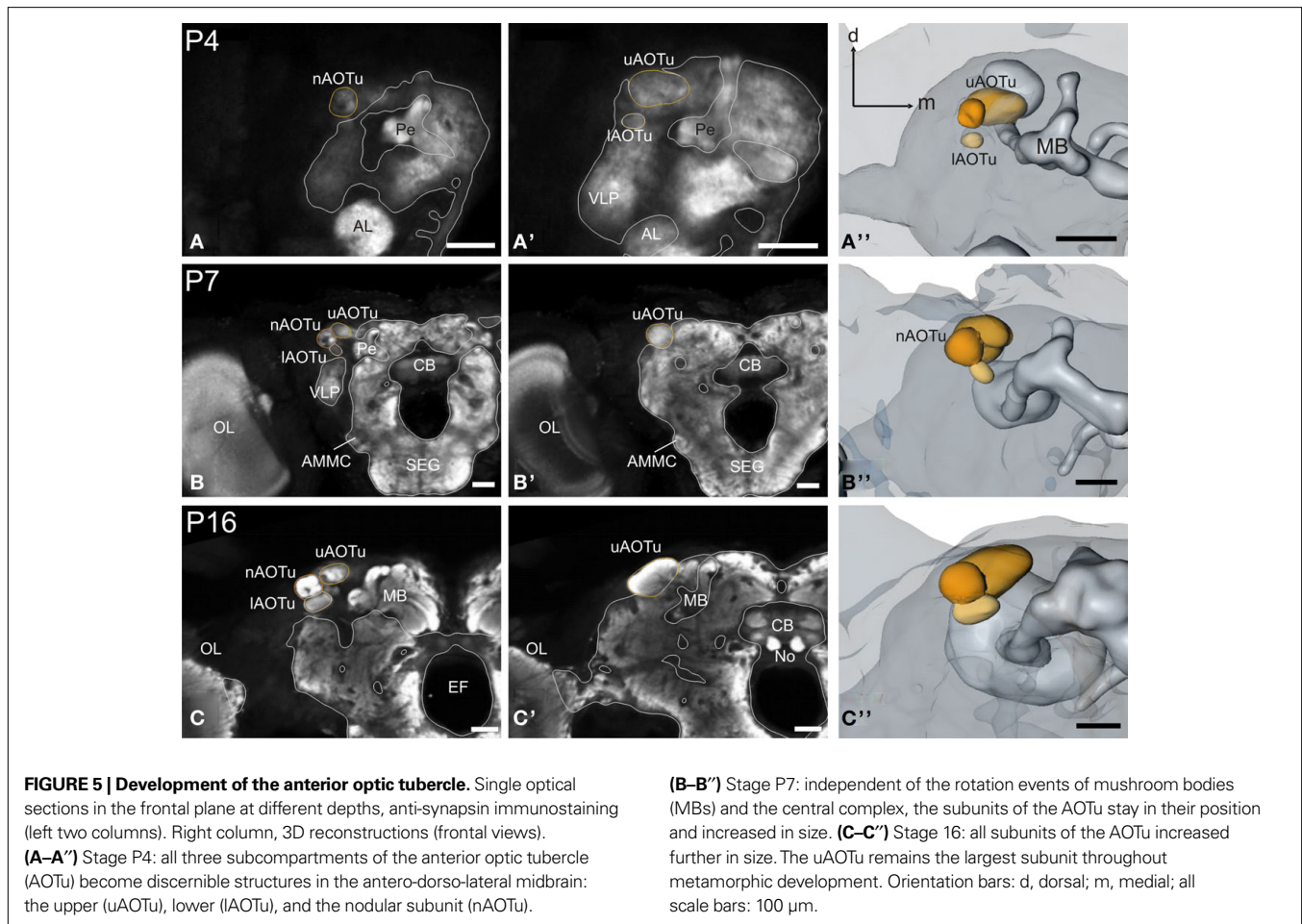
of pupal development exhibit neither major structural changes nor additional translational movements of neuropils, but rather massive increase in size.

Analysis of the volume increases of each of the examined neuropils reveals that all neuropils start with massive growth at around stage P3/P4 (Figure 7). Thus, in contrast to the onset of the synapsin signal, which differed between the neuropils, the onset of the massive volume increase starts at about the same developmental time for all neuropils.

#### 4D VISUALIZATION IN CINEMA 4D

To summarize all described changes in relation to position, shape and size of the individual neuropils, we generated an animation of the metamorphosing *M. sexta* female brain (Movie S1 in Supplementary Material). As an initial point of the animation we choose the last instar brain (L5) and animated the development of

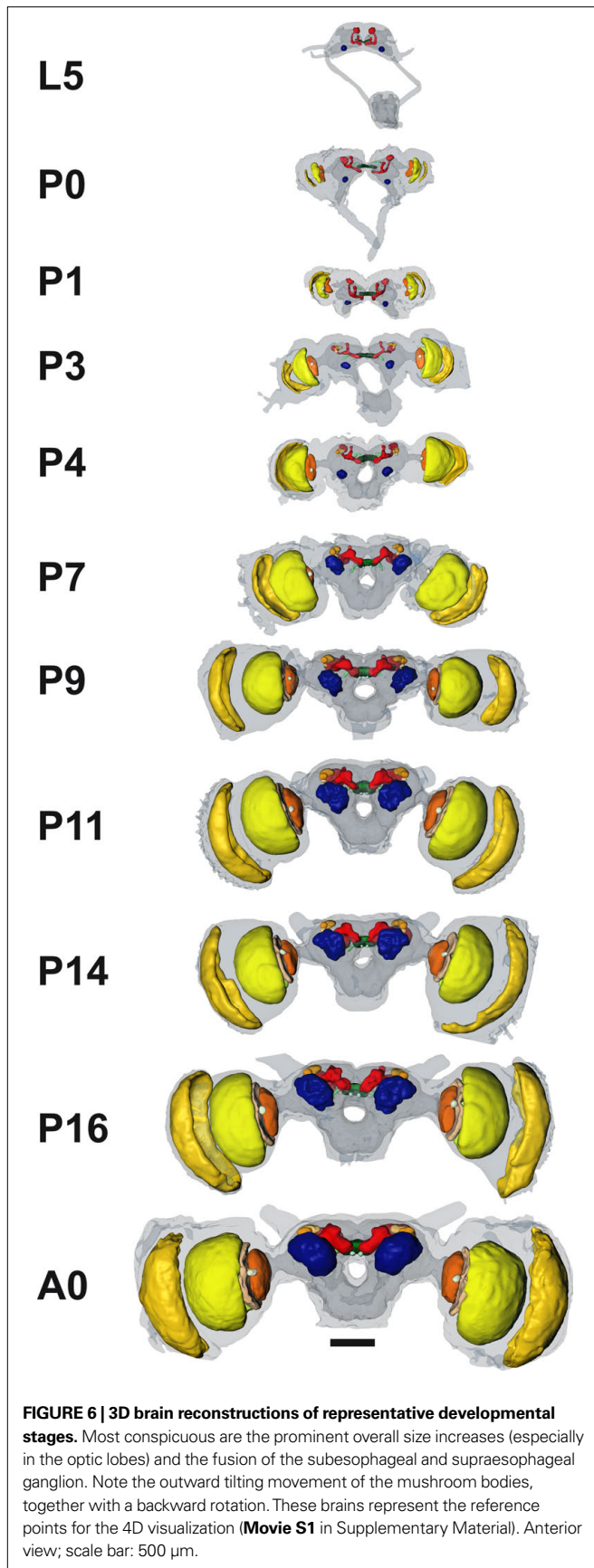
the brain during metamorphosis until the adult stage A0. For the 4D visualization, we animated the development of the individual neuropils including their subunits and additionally the brain surfaces which we also labeled during 3D reconstructions and which were also standardized in the *M. sexta* standard brain (el Jundi et al., 2009). For the animation of individual neuropils and the brain surface we used the 3D reconstructed surface models which were for each developmental stage created in Amira (Figure 9). Beside these individual brains we also used as the final point of the animation the female standard brain of *M. sexta* (el Jundi et al., 2009). To ease calculations we reduced the number of the polygons of the surface models in AMIRA and exported every brain as drawing exchange format (.dxf) file. The surface models or brain polygon models of the selected brains which are shown in Figure 6 were then imported in the software program Cinema 4D where the virtual animation of the brain development was generated. To further simplify the



necessary calculations in the software, only one brain hemisphere of the bilateral symmetrical *M. sexta* brain (except the subunits of the central body) was animated and subsequently mirrored for the movie. Also, pedunculus and calyx were integrated to one polygonal model with the tool *Connect*. Next we defined the length of the animation using the taskbar *Timeline* (Figure 9). To attribute crucial substages (i.e. P7/8), the timeline was subdivided in 41 “stages”, each 35 frames long, thus giving 1435 frames for the 4D animation. To define the L5 larval brain as the initial brain, we selected this brain and set a *Key* in the timeline at frame 0 (Figure 9). Basic structures with only few polygons like a sphere can easily be morphed in a cube with the module *Morph*. Because of the complexity of the neuropil structures it was not possible to create the 4D visualization with this module. During the animation the program does not allow a change of the number of polygons. Because some adult neuropils are not present in the larval brain, we first scaled down the adult brain onto the larval brain and reduced non-existent neuropils to point-size. This downscaled brain, adapted to fit the shape of the L5 brain, was then used as a starting point for the subsequent morphing process. All neuropils of all brains were displayed as grid polygonal models using the tool *Display*, except of the starting brain which was displayed as a polygonal surface model (Figure 9A). During the morphing process, only the starting brain, which was morphed from one stage to the next, and the brain of the next

corresponding developmental step were visible. With the tool *Model* the localization of every neuropil of the starting brain was positioned approximately in the center of the corresponding neuropil in the brain of the next reconstructed developmental stage. These positional changes of individual neuropils were then saved by setting a *Key* in the *Timetable* to the adequate frame number. Then the polygon edges were made selectable with the tool *Point Selection* and with the tool *Magnet* the polygons of every neuropil of the starting brain were manually adapted to fit the polygons of the neuropil of the next reconstructed brain in the developmental timeline. Changes in size and shape of the neuropils were again saved by a *Key* in the *Timetable*. Beside this changes in shape and size we also rotated the structures, for example the mushroom bodies. For every modification (scaling, rotating, positioning and shaping) a *Key* was set in the *Timeline* and the neuropils of the starting brain were slowly morphed step by step to eventually match the adult A0 brain. The temporal progress in relation to size, rotation and position of the structures between two *Keys* is sigmoid by default in Cinema 4D (Figure 9B). The temporal progress of the rotation, scale and position of the animation between all *Keys* is visible in the *Timeline* window as f-curves. To better fit the observed developmental changes between the stages into the temporal progress, we used additional *Keys* between these *Keys* in the f-curves (Figure 9B’). After creation of the 4D visualization we exported the 1435 images





from Cinema 4D as Targa image file format (.tga). Thereby image data were rendered with  $1280 \times 1024$  pixel resolution. To obtain a high-quality animation of brain development we imported these 1435 images in the freeware Virtual Dub (v. 1.9.7., <http://www.virtualdub.org>) and created an Audio Video Interleave file (.avi) movie. Thereby we defined the frame rate to 25 frames per second, so that the 4D animation of the brain development has a length of 57.4 s. To reduce the file size of this movie we converted this movie with a DIVX-converter to a divx-video format. The 4D animation of the brain development of *M. sexta* from anterior is shown in **Movie S1** in Supplementary Material.

## DISCUSSION

The development of a brain is a highly complex process in space and time. Eventually, all brain neuropils are formed, become located in their correct position and the connections between the neuropils are organized in a correct way. Owing to the amount of different neuropils and the different time lines, it is a challenge to envisage and may be even quantify such a process in its entirety. With the current paper, we present a feasibility study which offers a strategy to visualize the development of brain neuropils. For this purpose we 3D reconstructed selected brain neuropils of selected stages during brain metamorphosis of the sphinx moth *M. sexta* and transferred the 3D-surface data into the animation program Cinema 4D. Advances in imaging techniques, 3D reconstruction software, and computer power led to 3D reconstructions of many brain areas and especially in insects led in some cases even to standardized brains to relate individual variations (*Drosophila melanogaster*: Rein et al., 2002; Jenett et al., 2006; the honeybee *Apis mellifera*: Brandt et al., 2005; the desert locust *Schistocerca gregaria*: Kurylas et al., 2008; two moth species: *M. sexta* (el Jundi et al., 2009) and *Heliothis virescens* (Kvella et al., 2009); the red flour beetle *Tribolium castaneum*: Dreyer et al., 2010). However, an animation of developing brain areas based on 3D-reconstructions from consecutive developmental stages has so far not been produced.

Development of most of the brain areas of *M. sexta* that we reconstructed has been described under various aspects in several publications over the years. In the following discussion, we first want to briefly compare the results of our study with the published data and then evaluate the used strategy and technique for a better understanding of developmental processes.

## OPTIC LOBES

The optic lobe is a highly retinotopically ordered neuropil that consists of three distinguishable neuropils, most distally the lamina, followed by the medulla and the lobula complex (Bullock and Horridge, 1965; Strausfeld, 1976; Homberg, 1994). In *M. sexta*, the optic anlagen, from which the optic lobes develop, are readily apparent in the third larval instar (Monsma and Booker, 1996). Similar to other insects, the outer optic anlagen give rise to the neurons of the lamina and the medulla and the inner optic anlagen give rise to the neurons forming the lobula neuropils (Nordlander and Edwards, 1969). Faint synapsin immunostaining revealed the presence of the lamina, medulla, and lobula at stage P0. As we did not reconstruct brains of late wandering larva, these neuropils could have been present already earlier. At stage P3 the lobula plate appears and additionally the intensity of the synapsin staining increased

in all optic neuropils including clear layers within the medulla. This result suggests that massive synaptogenesis starts around P3 which is very likely correlated with the incoming axons of the photoreceptor cells starting at P2/3 (Monsma and Booker, 1996). An earlier study, which postulated expression of superoxide dismutase (SOD) as an indicator for neurons forming their synapses, found high levels of transient SOD staining in many optic lobe neurons starting around stage P2/3 and ending at different times during metamorphic development (Schachtner et al., 2004a). In parallel to the increasing synapsin and SOD signal, the optic neuropils start from stage P3 with a more or less linear growth up to adult size (A0, Figure 7). Regulated by the increasing hemolymph titer of 20-hydroxyecdysone, mitotic activity in the outer optic anlagen abruptly ceases at P6 with some mitotic cells up to P10 and from P8 to P10 neuroblasts of the outer optic anlagen undergo programmed cell death (Monsma and Booker, 1996; Champlin and Truman, 1998b). Also, the last axons of retinal photoreceptor axons reach the lamina at stage P6 (Monsma and Booker, 1996). In summary, these data suggest that the linear increase of the lamina and the medulla volumes between P3 and P6 is driven by several factors including ingrowing axons of photoreceptor cells from the retina, synaptogenesis between the different partners, general neuronal

growth, and neurogenesis. The stop of photoreceptor axon arrival and the abrupt cease of neurogenesis are not mirrored in the observed growth rate. Thus, the linear growth following stage P6 must be driven by other mechanisms which reflect the maturation of the neuronal network within lamina and medulla.

The adult accessory medulla is connected to the adult remnants of the larval photoreceptors, the stemmata (Lampel et al., 2005), pointing towards the larval optic neuropils as developmental origin of the accessory medulla. This larval origin was claimed for *Papilio* (Ichikawa, 1994); an idea originally brought up for the accessory lamina and medulla in neuropteroids (Ehnborn, 1948).

**ANTENNAL LOBES**

The paired antennal lobes (ALs) are the first central integration centers for the odor information in the insect brain (reviewed in Schachtner et al., 2005). During metamorphosis the adult ALs, which in *M. sexta* consist of about 60 olfactory glomeruli develop from an agglomerular larval antennal center (LAC; for a review see Tolbert et al., 2004). In *Drosophila* and in *M. sexta* the LAC is replaced by the adult AL (Kent et al., 1987; Jefferis et al., 2004). In both species, neuron populations which innervate the LAC persist through metamorphosis and build together with new born neurons the adult AL

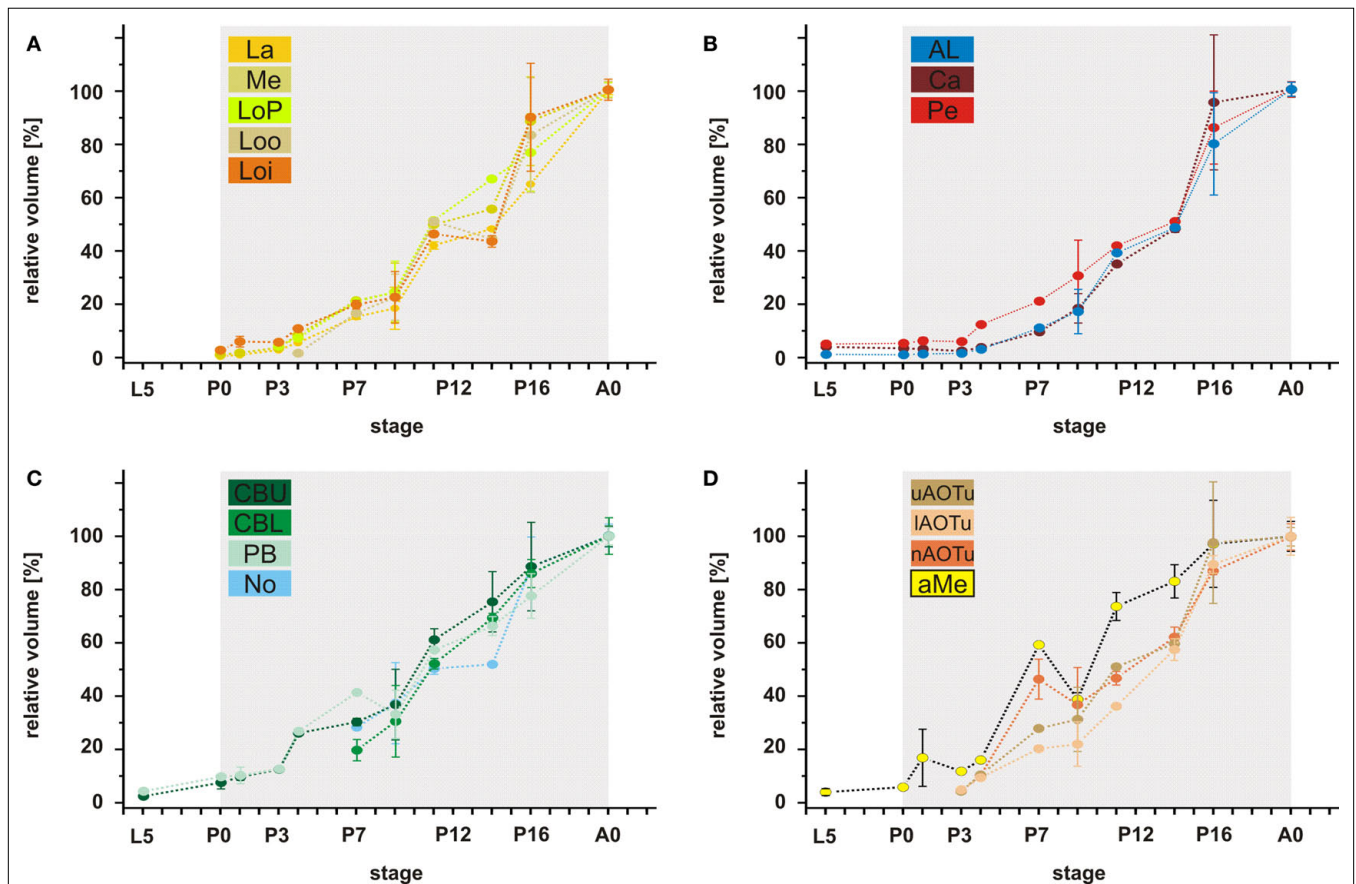


**FIGURE 7 | Relative volumes of the examined neuropils. (A)** The optic lobe neuropils; **(B)** The antennal lobes and the mushroom bodies; **(C)** The central complex; **(D)** The anterior optic tubercle and the accessory medulla. For each data point values of two brains are used (only for P4; n = 1). For bilateral neuropils, the means of the volumes of the individual animal were used.

Deviation bars, standard errors. La, lamina; Me, medulla; LoP, lobula plate; Loo, outer lobula; Loi, inner lobula; AL, antennal lobe; Ca, calyx; Pe, pedunculus; CBU, upper unit of the central body (CB); CBL, lower unit of the CB; PB, protocerebral bridge; No, nodule; uAOTu, upper anterior optic tubercle (AOTu); lAOTu, lower AOTu; nAOTu, nodular subunit of the AOTu; a Me, accessory medulla.

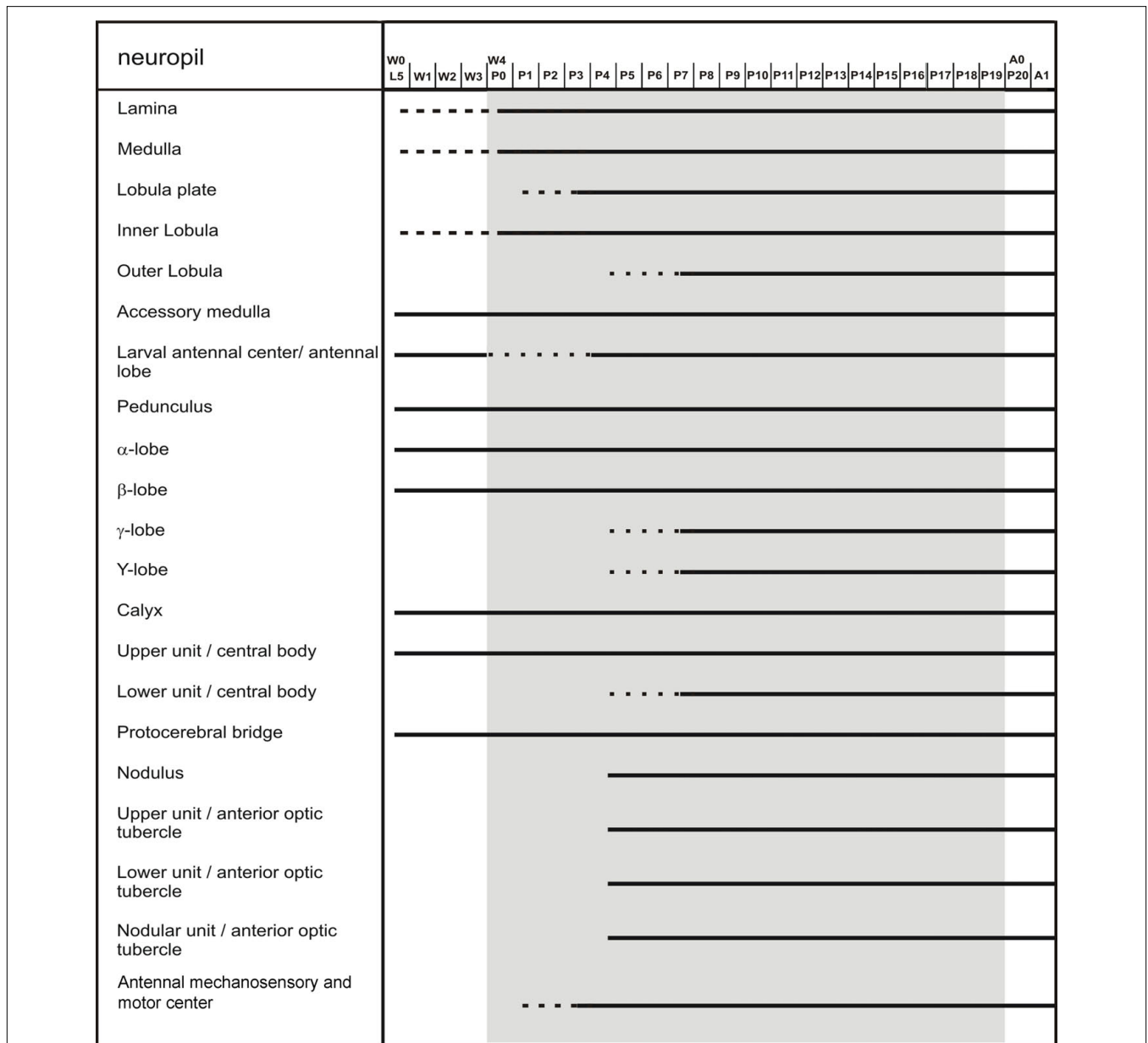
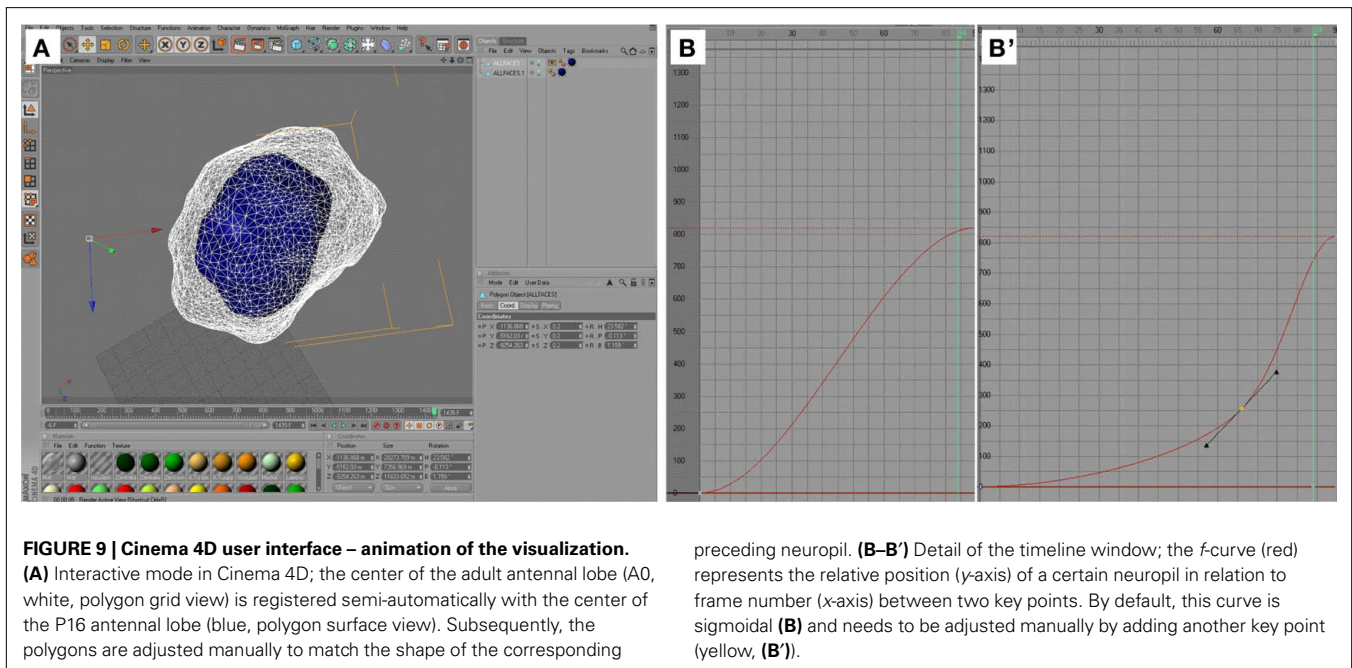


**FIGURE 8 | Scheme of brain neuropil development.** The scheme, based on anti-synapsin immunostaining, reflects the developmental time course of the individual neuropils. Dotted lines represent the gradual appearance of a neuropil, or, in case of the larval antennal center, its transition into the antennal lobe.

circuit (Homborg and Hildebrand, 1994; Schachtner et al., 2004b; Marin et al., 2005; Utz and Schachtner, 2005; Utz et al., 2008). In a recent study the metamorphic development of the *M. sexta* ALs has been monitored using an antiserum against synaptotagmin, another ubiquitous synaptic vesicle protein (Dubuque et al., 2001). The findings of the current study using an anti-synapsin antiserum clearly resemble the findings of this earlier study. Dubuque et al. (2001) divided AL development into three phases. The preparation phase (phase I) lasts about 7–8 days beginning at pupal formation. It includes the birth of all AL neurons, the arrival of the axons of the olfactory receptor neurons from stage P3 to P10 in the ALs, and the formation of the protoglomeruli, the sites where the glomeruli form during phase II. The glomeruli formation phase (phase II)

lasts about 5 days and is characterized by massive synaptogenesis between the involved neurons. It is assumed, that during phase II a basic network of synaptic contacts within and between the glomeruli is established, which ensures the principal correlation of input and output components of the AL (Dubuque et al., 2001). In contrast to phase II, in phase III, which lasts about 8 days up to adult eclosion, only little synaptogenesis occurs. During this last phase, the glomeruli grow in size between 40 and 130% (Huetteroth and Schachtner, 2005). This is probably because of the increasing neurite diameters, and the synaptic wiring in the glomeruli is thought to undergo further refinement and maturation (Tolbert et al., 1983; Tolbert, 1989; Dubuque et al., 2001). The volume curve mirrors the three phases (Figure 7). Volume increase starts at stage P3. At



stage P7 the growth rate goes up and after P11/12, there seems to be a reduction in growth rate which is then increasing again. We are aware that we only reconstructed two brains per stage and that the results have to be judged under this prerequisite. An upward movement of the antennal lobes beginning at stage P3 has been described by Homberg and Hildebrand (1994). Our study gives a much more exact time course for this movement of the developing antennal lobes which starts at P3 and ends at stage P9.

### MUSHROOM BODIES

Mushroom bodies (MBs) are generally associated with higher integration processes and learning (e.g. Menzel, 2001; Heisenberg, 2003), but might also serve a general function in the control of behavior (e.g. Huber, 1955a,b; Erber et al., 1987; Zars, 2000; Strausfeld et al., 2009). In Lepidoptera larva, the opening of the MB calyces point to the dorsal surface of the brain and the  $\alpha$ -lobe is oriented frontally but in contrast to other insects the MBs rotate backwards during metamorphic development (Nordlander and Edwards, 1968; Homberg and Hildebrand, 1994). As expected from the description of Homberg and Hildebrand (1994), the dorsal rotation starts around stage P3. Our data reveal additionally that the MBs reach their adult position at P7. Growth of the pedunculi is nearly linear from P3 to adult eclosion. The calyces in contrast also start to increase their volumes, but cease growth between P9 and P14 before they reenter a growth rate similar to the growth rate before stage P9. Adult MBs are formed by adding new Kenyon cells to the larval MBs (e.g. Panov, 1957; Nordlander and Edwards, 1970; Technau and Heisenberg, 1982; Ito and Hotta, 1992; Lee et al., 1999; Zhao et al., 2008) and the larval Kenyon cells are reorganized during metamorphosis (e.g. Technau and Heisenberg, 1982; Ito and Hotta, 1992; Lee et al., 1999). Metamorphic MB development has so far not been examined in *M. sexta* and thus, it is not known when neurogenesis and reorganization of larval neurons occur. Schachtner et al. (2004a) described strong SOD expression starting

around stage P3/4 and ending at stage P16. The SOD expression occurs in different Kenyon cell clusters and might indicate synapse formation between the different Kenyon cells during this time. After P16, other factors than synaptogenesis might be responsible for the neuropil growth.

### OTHER NEUROPILS OF THE CNS

The role of the central complex still remains elusive, but is probably best described as a central coordinating center in sensory and motor integration (for reviews see Strauss, 2002; Wessnitzer and Webb, 2006; Homberg, 2008). The central complex consists of the central body (CB) and the protocerebral bridge (PB), which are both already present in the *M. sexta* larva (Granger et al., 1989; Homberg and Hildebrand, 1994). However, the metamorphic development of the central complex in *M. sexta* has not been described so far. In contrast to adults, the larval CB consists only of an upper unit (CBU; Homberg and Hildebrand, 1994). This is consistent with larval CB morphology in other insects, including e.g. another moth, the honey bee (*Antheraea pernyi*, *Apis mellifera*: Panov, 1959) and two beetles (*Tenebrio molitor*: Panov, 1959; Wegerhoff and Breidbach, 1991; *Tribolium castaneum*: personal observation). Our reconstructions clearly show that the lower unit of the CB (CBL) forms between P4 and P7. Additionally, the CB and the PB rotate backwards, thus positioning the CBL anteriorly to the CBU and the PB behind the CB. This orientation is eventually reached at stage P7 and remains up to adulthood. Like other examined neuropils, the volumes of all central complex neuropils start their metamorphic growth around stage P3.

The anterior optic tubercle (AOTu) including all subunits forms around stage P4. To date, only sparse information about the functional role of the AOTu is present, but in locusts it receives input from the optic lobes (Homberg et al., 2003). Since optic lobe development precedes AOTu development, the formation of the AOTu might be initiated by subsequent afferent innervation from there.

### HORMONAL REGULATION OF METAMORPHIC BRAIN DEVELOPMENT

The major developmental hormones in insects are the juvenile hormones and the ecdysteroids. Interaction between these hormones causes the switch from larval to pupal development in holometabolous insects (for a recent review see Truman, 2009). In *M. sexta*, the major circulating ecdysteroid during metamorphosis is 20-hydroxyecdysone (20E; Warren and Gilbert, 1986). Effects of 20E on metamorphic development of the nervous system of *M. sexta* have been shown in several studies: the pupal 20E peak regulates the fusion of thoracic and abdominal ganglia (Amos et al., 1996), it controls cell proliferation during genesis of the optic lobes and the retina but also programmed cell death of optic lobe neuroblasts (Champlin and Truman, 1998a,b, 2000), and the onset of the formation of the olfactory glomeruli (Schachtner et al., 2004a). The pupal 20E peak also regulates the pupal expression of tyramine  $\beta$ -hydroxylase, an essential enzyme for octopamine biosynthesis (Lehmann et al., 2000) and the expression of several neuropeptides in the developing AL (Schachtner et al., 2004b; Utz and Schachtner, 2005; Utz et al., 2008). The start of massive volume increase of all examined neuropils parallels the 20E hemolymph titer which starts to increase from stage P3 (Figure 7; Warren and Gilbert, 1986). This suggests that a low threshold of 20E is sufficient for the onset of differentiation and growth of most brain neuropils including newly formed neuropils but also persistent larval neuropils. In addition to the presence of 20E other signals are needed to coordinate the development of brain neuropils. For example, in *Manduca* and *Drosophila* ingrowing photoreceptor axons stimulate proliferation in the outer optic anlagen (Selleck and Steller, 1991; Huang and Kunes, 1996) and in the antennal lobe, ingrowing axons of the receptor neurons are needed to form the protoglomeruli, the templates for the later developing olfactory glomeruli (Oland and Tolbert, 1996). During ongoing pupal development, higher 20E thresholds are needed for further neuropil specific differentiation like the stop of mitosis and the start of neuroblast apoptosis in the outer optic anlagen (Champlin and Truman, 1998b) or the onset of glomerulus formation in the AL (Schachtner et al., 2004b).

### 3D DIGITAL BRAIN ATLASES AND 4D ANIMATION

This study provides 3D reconstructions of defined neuropils at different stages during metamorphosis of the sphinx moth brain. These 3D reconstructions were then used to produce a digital animation which visualizes the development of the individual neuropils in context to each other. *M. sexta* has been used for decades as a model to study metamorphic brain development but so far no anatomical atlases comparing form, volume, and position of neuropils at different metamorphic stages were available. Our study adds this anatomical information in a digital form and the 3D data sets can be provided on request. A comparison between published data on metamorphic brain development (see above) and our study clearly revealed additional new information e.g. detailed positional information and information on volume increases along the developmental timeline. Data sets like the one we provided here can be used as a basis for a growing digital framework in which all available information on different developmental steps can be provided. This can include anatomical data, ranging from gross anatomy to single cells, but

also experimental data of any kind including physiological and even genetical data. The advantage of digital brain atlases or databases has been recognized by the research community and meanwhile such atlases have been introduced for vertebrate and invertebrate brains serving a wide range of purposes in basic research, but its importance also in applied medicine are obvious. For example, digital brain atlases of the human brain are available mainly based on MRI but also an increasing set of other data sources, storing information on brain variations across age and gender, comparing brains in health and disease, and providing data in large human populations (for recent reviews see Toga and Thompson, 2001; Toga et al., 2006). Among other interesting approaches including e.g. pest control and evolutionary questions, insects have a long tradition as models for basic questions in neuroscience ranging from the development of the nervous system to plasticity and memory formation. In this context digital atlases of certain insect models have been provided including standardized brains to relate individual variations. These atlases are intended as frameworks to allow the mapping of neurons provided by different researchers (Brandt et al., 2005; Kurylas et al., 2008; Kvello et al., 2009; el Jundi et al., 2010), to study genetical variations (Rein et al., 2002; Jenett et al., 2006), and in general developmental and adult plasticity (el Jundi et al., 2009; Dreyer et al., 2010). One example which nicely demonstrates the usefulness of such atlases are maps of the olfactory glomeruli of certain insects which serve as tools to study development, function and plasticity of the glomerular network (e.g. Galizia et al., 1999; Sachse and Galizia, 2003; Fishilevich and Vosshall, 2005; Skiri et al., 2005; Deisig et al., 2006; Zhang et al., 2006; Root et al., 2007; Sachse et al., 2007; Riffell et al., 2009; Staudacher et al., 2009; Varela et al., 2009).

One major advantage of 4D visualization is clearly the didactical value; watching the animated brain development allows for better comprehension of neuropil growth and movement in its temporal context. This is not only helpful for researchers coming from a different organism and who want to compare developmental processes, but also for beginners in the field and last but not least for students. Owing to increasing computer power, internet bandwidth, and accessibility, digital databases of brain architecture and function including development and 4D visualization will in the future be accessible in an interactive way via web based access. Ideally, this access is then provided via ontologies, which allows the use of these data bases not only for the specialists but also for other researchers and students.

### ACKNOWLEDGMENTS

The authors thank Dr. Erich Buchner (University of Würzburg, Germany) for kindly providing the anti-synapsin antibody. The authors are also grateful to Dr. Uwe Homberg for many fruitful discussions, and Martina Kern and Torsten Bauschke for expert technical assistance. This work was supported by a DFG grant (SCHA 678/3-3) to Joachim Schachtner.

### SUPPLEMENTARY MATERIAL

The Supplementary Material for this article can be found online at <http://www.frontiersin.org/systemsneuroscience/paper/10.3389/fnsys.2010.00007/>

## REFERENCES

- Amos, T. M., Gelman, D. B., and Mesce, K. A. (1996). Steroid hormone fluctuations regulate ganglionic fusion during metamorphosis of the moth *Manduca sexta*. *J. Insect Physiol.* 42, 579–591.
- Amos, T. M., and Mesce, K. A. (1994). Reorganization of the ventral nerve cord in the moth *Manduca sexta* (L.) (Lepidoptera: Sphingidae). *Int. J. Insect Morphol. Embryol.* 23, 21–37.
- Bell, R. A., and Joachim, F. A. (1978). Techniques for rearing laboratory colonies of the tobacco hornworm, *Manduca sexta*, and pink ballworms. *Ann. Entomol. Soc. Am.* 69, 365–373.
- Brandt, R., Rohlfing, T., Rybak, J., Kroczyk, S., Maye, A., Westerhoff, M., Hege, H. C., and Menzel, R. (2005). Three-dimensional average-shape atlas of the honeybee brain and its applications. *J. Comp. Neurol.* 492, 1–19.
- Bullock, T. H., and Horridge, G. A. (1965). Structure and Function in the Nervous Systems of Invertebrates, Vol. 2. San Francisco, Freeman.
- Champlin, D. T., and Truman, J. W. (1998a). Ecdysteroid control of cell proliferation during optic lobe neurogenesis in the moth *Manduca sexta*. *Development* 125, 269–277.
- Champlin, D. T., and Truman, J. W. (1998b). Ecdysteroids govern two phases of eye development during metamorphosis of the moth, *Manduca sexta*. *Development* 125, 2009–2018.
- Champlin, D. T., and Truman, J. W. (2000). Ecdysteroid coordinates optic lobe neurogenesis via a nitric oxide signaling pathway. *Development* 127, 3543–2551.
- Deisig, N., Giurfa, M., Lachnit, H., and Sandoz, J.-C. (2006). Neural representation of olfactory mixtures in the honeybee antennal lobe. *Eur. J. Neurosci.* 24, 1161–1174.
- Dreyer, D., Vitt, H., Dippel, S., Goetz, B., el Jundi, B., Kollmann, M., Huetteroth, W., and Schachtner, J. (2010). 3D standard brain of the red flour beetle *Tribolium castaneum*: a tool to study metamorphic development and adult plasticity. *Front. Syst. Neurosci.* 4:3. doi: 10.3389/neuro.06.003.2010
- Dubuque, S. H., Schachtner, J., Nighorn, A. J., Menon, K. P., Zinn, K., and Tolbert, L. P. (2001). Immunolocalization of synaptotagmin for the study of synapses in the developing antennal lobe of *Manduca sexta*. *J. Comp. Neurol.* 441, 277–287.
- Ehnborn, K. (1948). Studies on the central and sympathetic nervous system and some sense organs in the head of neuropteroid insects. *Opusc. Entomol. (Suppl.)* 8, 1–162.
- el Jundi, B., Heinze, S., Lenschow, C., Kurylas, A., Rohlfing, T., and Homberg, U. (2010). The locust standard brain: a 3D standard of the central complex as a platform for neural network analysis. *Front. Syst. Neurosci.* 3:21. doi: 10.3389/neuro.06.021.2009
- el Jundi, B., Huetteroth, W., Kurylas, A. E., and Schachtner, J. (2009). Anisometric brain dimorphism revisited: implementation of a volumetric 3D standard brain in *Manduca sexta*. *J. Comp. Neurol.* 517, 210–225.
- Erber, J., Homberg, U., and Gronenberg, W. (1987). Functional roles of the mushroom bodies in insects. In *Arthropod Brain: Its Evolution, Development, Structure, and Functions*, A. P. Gupta, ed. (New York, Wiley), pp. 485–511.
- Fishilevich, E., and Vosshall, L. B. (2005). Genetic and functional subdivision of the *Drosophila* antennal lobe. *Curr. Biol.* 15, 1548–1553.
- Galizia, C. G., Sachse, S., Rappert, A., and Menzel, R. (1999). The glomerular code for odor representation is species specific in the honeybee *Apis mellifera*. *Nature* 2, 473–478.
- Granger, N. A., Homberg, U., Henderson, P., Towle, A., and Lauder, J. M. (1989). Serotonin-immunoreactive neurons in the brain of *Manduca sexta* during larval development and larval-pupal metamorphosis. *Int. J. Dev. Neurosci.* 7, 55–72.
- Grimaldi, D., and Engel, M. S. (2005). *Evolution of the Insects*. Cambridge, Cambridge University Press.
- Heisenberg, M. (2003). Mushroom body memoir: from maps to models. *Nat. Rev. Neurosci.* 4, 266–275.
- Homberg, U. (1994). Distribution of Neurotransmitters in the Insect Brain. *Progress in Zoology* 40; Stuttgart, Fischer.
- Homberg, U. (2008). Evolution of the central complex in the arthropod brain with respect to the visual system. *Arthropod Struct. Dev.* 37, 347–362.
- Homberg, U., and Hildebrand, J. G. (1994). Postembryonic development of gamma-aminobutyric acid-like immunoreactivity in the brain of the sphinx moth *Manduca sexta*. *J. Comp. Neurol.* 339, 132–149.
- Homberg, U., Hofer, S., Pfeiffer, K., and Gebhardt, S. (2003). Organization and neural connections of the anterior optic tubercle in the brain of the locust, *Schistocerca gregaria*. *J. Comp. Neurol.* 462, 415–430.
- Huang, Z., and Kunes, S. (1996). Hedgehog, transmitted along retinal axons, triggers neurogenesis in the developing visual centers of the *Drosophila* brain. *Cell* 86, 411–422.
- Huber, F. (1955a). Über die Funktion der Pilzkörper (*Corpora pedunculata*) beim Gesang der Keuleneuschrecke *Gomphocerus rufus* L. (Acridiidae). *Naturwissenschaften* 20, 566–567.
- Huber, F. (1955b). Sitz und Bedeutung nervöser Zentren für Instinkthandlungen beim Männchen von *Gryllus campestris* L. *Z. Tierpsychol.* 12, 12–48.
- Huetteroth, W., and Schachtner, J. (2005). Standard three-dimensional glomeruli of the *Manduca sexta* antennal lobe: a tool to study both developmental and adult neuronal plasticity. *Cell Tissue Res.* 319, 513–524.
- Ichikawa, T. (1994). Reorganization of visual interneurons during metamorphosis in the swallowtail butterfly *Papilio xuthus*. *J. Comp. Neurol.* 340, 185–193.
- Ito, K., and Hotta, Y. (1992). Proliferation pattern of postembryonic neuroblasts in the brain of *Drosophila melanogaster*. *Dev. Biol.* 149, 134–148.
- Jefferis, G. S., Vyas, R. M., Berdnik, D., Ramaekers, A., Stocker, R. F., Tanaka, N. K., Ito, K., and Luo, L. (2004). Developmental origin of wiring specificity in the olfactory system of *Drosophila*. *Development* 131, 117–130.
- Jenett, A., Schindelin, J. E., and Heisenberg, M. (2006). The Virtual Insect Brain Protocol: Creating and Comparing Standardized Neuroanatomy. *BMC Bioinformatics* 7, 544.
- Jindra, M., Huang, J. Y., Malone, F., Asahina, M., and Riddiford, L. M. (1997). Identification and mRNA developmental profiles of two ultraspiracle isoforms in the epidermis and wings of *Manduca sexta*. *Insect Mol. Biol.* 6, 41–53.
- Kent, K. S., Hoskins, S. G., and Hildebrand, J. G. (1987). A novel serotonin-immunoreactive neuron in the antennal lobe of the sphinx moth *Manduca sexta* persists throughout postembryonic life. *J. Neurobiol.* 18, 451–465.
- Klagges, B. R., Heimbeck, G., Godenschwege, T. A., Hofbauer, A., Pflugfelder, G. O., Reifegerste, R., Reisch, D., Schaupp, M., Buchner, S., and Buchner, E. (1996). Invertebrate synapsins: a single gene codes for several isoforms in *Drosophila*. *J. Neurosci.* 16, 3154–3165.
- Kurylas, A. E., Rohlfing, T., Kroczyk, S., Jenett, A., and Homberg, U. (2008). Standardized atlas of the brain of the desert locust, *Schistocerca gregaria*. *Cell Tissue Res.* 333, 125–145.
- Kvella, P., Lövaldli, B. B., Rybak, J., Menzel, R., and Mustaparta, H. (2009). Digital, three-dimensional average shaped atlas of the *Heliothis virescens* brain with integrated gustatory and olfactory neurons. *Front. Syst. Neurosci.* 3:14. doi: 10.3389/neuro.06.014.2009
- Lampel, J., Briscoe, A. D., and Wasserthal, L. T. (2005). Expression of UV-, blue-, long-wavelength-sensitive opsins and melatonin in extraretinal photoreceptors of the optic lobes of hawk moths. *Cell Tissue Res.* 321, 443–458.
- Lee, T., Lee, A., and Luo, L. (1999). Development of the *Drosophila* mushroom bodies: sequential generation of three distinct types of neurons from a neuroblast. *Development* 126, 4065–4076.
- Lehman, H. K., Klukas, K. A., Gilchrist, L. S., and Mesce, K. A. (2000). Steroid regulation of octopamine expression during metamorphic development of the moth *Manduca sexta*. *J. Comp. Neurol.* 424, 283–296.
- Marin, E. C., Watts, R. J., Tanaka, N. K., Ito, K., and Luo, L. (2005). Developmentally programmed remodeling of the *Drosophila* olfactory circuit. *Development* 132, 725–737.
- Menzel, R. (2001). Searching for the memory trace in a mini-brain, the honeybee. *Learn. Mem.* 8, 53–62.
- Monisma, S. A., and Booker, R. (1996). Genesis of the adult retina and outer optic lobes of the moth, *Manduca sexta*. I. Patterns of proliferation and cell death. *J. Comp. Neurol.* 367, 10–20.
- Nordlander, R. H., and Edwards, J. S. (1968). Morphology of the larval and adult brains of the monarch butterfly, *Danaus plexippus plexippus*, L. *J. Morphol.* 126, 67–94.
- Nordlander, R. H., and Edwards, J. S. (1969). Postembryonic brain development in the monarch butterfly, *Danaus plexippus plexippus*, L. II. The optic lobe. *Wilhelm Roux Arch. Entwickl. Mech. Org.* 163, 197–220.
- Nordlander, R. H., and Edwards, J. S. (1970). Postembryonic brain development in the monarch butterfly, *Danaus plexippus plexippus* L. III. Morphogenesis of centers other than the optic lobes. *Wilhelm Roux Arch. Entwickl. Mech. Org.* 164, 247–260.
- Oland, L. A., and Tolbert, L. P. (1996). Multiple factors shape development of olfactory glomeruli: insights from an insect model system. *J. Neurobiol.* 30, 92–109.
- Otsuna, H., and Ito K. (2006). Systematic analysis of the visual projection neurons of *Drosophila melanogaster*. I. Lobula-specific pathways. *J. Comp. Neurol.* 497, 928–958.
- Panov, A. A. (1957). The structure of the brain in insects in successive stages of postembryonic development. *Rev. Entomol. U.R.S.S.* 36, 269–284.
- Panov, A. A. (1959). The structure of the insect brain at successive stages of postembryonic development. II. The central body. *Rev. Entomol. U.R.S.S.* 38, 276–284.

- Rein, K., Zöckler, M., Mader, M. T., Grübel, C., and Heisenberg, M. (2002). The *Drosophila* standard brain. *Curr. Biol.* 12, 227–231.
- Riffell, J. A., Lei, H., Christensen, T. A., and Hildebrand, J. G. (2009). Characterization and coding of behaviorally significant odor mixtures. *Curr. Biol.* 19, 335–340.
- Root, C. M., Semmelhack, J. L., Wong, A. M., Flores, J., and Wang, J. W. (2007). Propagation of olfactory information in *Drosophila*. *Proc. Natl. Acad. Sci. U.S.A.* 104, 11826–11831.
- Sachse, S., and Galizia, C. G. (2003). The coding of odour-intensity in the honeybee antennal lobe: local computation optimizes odour representation. *Eur. J. Neurosci.* 18, 2119–2132.
- Sachse, S., Rueckert, E., Keller, A., Okada, R., Tanaka, N. K., Ito, K., and Vosshall, L. B. (2007). Activity-dependent plasticity in an olfactory circuit. *Neuron* 56, 838–850.
- Schachtner, J., Huetteroth, W., Nighorn, A., and Honegger, H. W. (2004a). Copper/zinc superoxide dismutase-like immunoreactivity in the metamorphosing brain of the sphinx moth *Manduca sexta*. *J. Comp. Neurol.* 469, 141–152.
- Schachtner, J., Trosowski, B., D'Hanis, W., Stubner, S., and Homberg, U. (2004b). Development and steroid regulation of RFamide immunoreactivity in antennal lobe neurons of the sphinx moth *Manduca sexta*. *J. Exp. Biol.* 207, 2389–2400.
- Schachtner, J., Schmidt, M., and Homberg, U. (2005). Organization and evolutionary trends of primary olfactory brain centers in Tetraconata (Crustacea + Hexapoda). *Arthropod Struct. Dev.* 34, 257–299.
- Schwartz, L. M., and Truman, J. W. (1983). Hormonal control of rates of metamorphic development in the tobacco hornworm *Manduca sexta*. *Dev. Biol.* 99, 103–114.
- Selleck, S. B., and Steller, H. (1991). The influence of retinal innervation on neurogenesis in the first optic ganglion of *Drosophila*. *Neuron* 6, 83–99.
- Skiri, H. T., Rø, H., Berg, B. G., and Mustaparta, H. (2005). Consistent organization of glomeruli in the antennal lobes of related species of heliothine moths. *J. Comp. Neurol.* 491, 376–380.
- Staudacher, E. M., Huetteroth, W., Schachtner, J., and Daly, K. C. (2009). A 4-dimensional representation of antennal lobe output based on an ensemble of characterized projection neurons. *J. Neurosci. Methods* 180, 208–223.
- Strausfeld, N. J. (1976). Atlas of an Insect Brain. Berlin, Springer.
- Strausfeld, N. J., Sinakevitch, I., Brown, S. M., and Farris, S. M. (2009). Ground plan of the insect mushroom body: functional and evolutionary implications. *J. Comp. Neurol.* 513, 265–291.
- Strauss, R. (2002). The central complex and the genetic dissection of locomotor behaviour. *Curr. Opin. Neurobiol.* 12, 633–638.
- Technau, G., and Heisenberg, M. (1982). Neural reorganization during metamorphosis of the corpora pedunculata in *Drosophila melanogaster*. *Nature* 295, 405–407.
- Toga, A. W., and Thompson, P. M. (2001). Maps of the brain. *Anat. Rec.* 265, 37–53.
- Toga, A. W., Thompson, P. M., Mori, M., Amunts, K., and Zilles, K. (2006). Towards multimodal atlases of the human brain. *Nat. Rev. Neurosci.* 7, 953–966.
- Tolbert, L. P. (1989). Afferent axons from the antenna influence the number and placement of intrinsic synapses in the antennal lobes of *Manduca sexta*. *Synapse* 3, 83–95.
- Tolbert, L. P., Matsumoto, S. G., and Hildebrand, J. G. (1983). Development of synapses in the antennal lobes of the moth *Manduca sexta* during metamorphosis. *J. Neurosci.* 3, 1158–1175.
- Tolbert, L. P., Oland, L. A., Tucker, E. S., Gibson, N. J., Higgins, M. R., and Lipscomb, B. W. (2004). Bidirectional influences between neurons and glial cells in the developing olfactory system. *Prog. Neurobiol.* 73, 73–105.
- Truman, J. W. (1996). Metamorphosis of the insect nervous system. In *Metamorphosis: Postembryonic Reprogramming of Gene Expression in Amphibian and Insect Cells*, L. I. Gilbert, ed. (Orlando, Academic Press), pp. 283–320.
- Truman, J. W. (2009). Hormonal control of the form and function of the nervous system. In *Insect Development: Morphogenesis, Molting and Metamorphosis*, L. I. Gilbert, ed. (London, Academic Press) pp. 133–162.
- Utz, S., Huetteroth, W., Vömel, M., and Schachtner, J. (2008). Mas-allatotropin in the developing antennal lobe of the sphinx moth *Manduca sexta*: distribution, time course, developmental regulation, and colocalization with other neuropeptides. *Dev. Neurobiol.* 68, 123–142.
- Utz, S., and Schachtner, J. (2005). Development of A-type allatostatin immunoreactivity in antennal lobe neurons of the sphinx moth *Manduca sexta*. *Cell Tissue Res.* 320, 149–162.
- Varela, N., Couton, L., Gemenio, C., Avilla, J., Rospars, J. P., and Anton, S. (2009). Three-dimensional antennal lobe atlas of the oriental fruit moth, *Cydia molesta* (Busck) (Lepidoptera: Tortricidae): comparison of male and female glomerular organization. *Cell Tiss. Res.* 337, 513–526.
- Warren, J. T., and Gilbert, L. I. (1986). Ecdysone metabolism and distribution during the pupal–adult development of *Manduca sexta*. *Insect Biochem.* 16, 65–82.
- Weevers, R. D. (1966). A lepidopteran saline: the effects of inorganic cation concentrations on sensory, reflex and motor responses in a herbivorous insect. *J. Exp. Biol.* 44, 163–176.
- Wegerhoff, R. and Breidbach, O. (1991). Distribution of GABA-like immunoreactivity throughout postembryogenesis of the midbrain in the beetle *Tenebrio molitor* L. (Insecta; Coleoptera). In *Synapse-Transmission and Modulation*, N. Elsner and H. Penzlin, eds (Stuttgart, Thieme), p. 158.
- Wessnitzer, J., and Webb, B. (2006). Multimodal sensory integration in insects – towards insect brain control architectures. *Bioinspir. Biomim.* 1, 63–75.
- Zars, T. (2000). Behavioral functions of the insect mushroom bodies. *Curr. Opin. Neurobiol.* 10, 790–795.
- Zhang, D., Zhou, W., Yin, C., Chen, W., Ozawa, R., Ang, L.-H., Anandan, L., Aigaki, T., and Hing, H. (2006). Misexpression screen for genes altering the olfactory map in *Drosophila*. *Genesis* 44, 189–201.
- Zhao, X., Coptis, V., and Farris, S. M. (2008). Metamorphosis and adult development of the mushroom bodies of the red flour beetle, *Tribolium castaneum*. *Dev. Neurobiol.* 68, 1487–1502.

**Conflict of Interest Statement:** The authors declare that the research was conducted in the absence of any commercial or financial relationship that could be construed as a potential conflict of interest.

Received: 16 November 2009; paper pending published: 29 December 2009; accepted: 21 February 2010; published online: 18 March 2010.

Citation: Huetteroth W, el Jundi B, el Jundi S and Schachtner J (2010) 3D-reconstructions and virtual 4D-visualization to study metamorphic brain development in the sphinx moth *Manduca sexta*. *Front. Syst. Neurosci.* 4:7. doi: 10.3389/fnsys.2010.00007

Copyright © 2010 Huetteroth, el Jundi, el Jundi and Schachtner. This is an open-access article subject to an exclusive license agreement between the authors and the Frontiers Research Foundation, which permits unrestricted use, distribution, and reproduction in any medium, provided the original authors and source are credited.